Supplementary Figure Legends

Supplementary Figure 1. Mass spectrometry (MS) analyses specifically identified PARP-1 in RECQ1-immunoprecipitates from HeLa nuclear extract. Immunoprecipitates using RECQ1 or normal rabbit IgG antibody were subjected to SDS-PAGE and stained with SYPRO Ruby. Corresponding gel slices from the RECQ1 and IgG-IP were subjected to in gel tryptic digestion prior to mass spectrometry analyses as described in materials and methods. Unique peptides of PARP-1 that were identified by MS/MS spectrum are indicated in bold.

Supplementary Figure 2. Immunoflurescence staining of endogenous RECQ1 and PARP-1. HeLa cells grown on coverslips were either mock treated or treated with 200 μM H_2O_2 for 10 min. We used a 1:100 dilution of mouse monoclonal PARP-1 antibody and a 1:500 dilution of rabbit polyclonal RECQ1 antibody, and immunoflurescence detection was performed as described [3]. Slides were analyzed with an LSM 510 Confocal Laser Scanning System. Immunostaining of RECQ1 (green), PARP-1 (red), and merged images of RECQ1 and PARP-1 are shown. DNA was stained by DAPI (4′,6′-diamidino-2-phenylindole).

Supplementary Figure 3. Coomassie stained gels showing recombinant RECQ1 and PARP-1 proteins. Lane 1 shows protein molecular weight marker as indicated.

Supplementary Figure 4. WRN-depleted cells show constitutive hyperactivation of PARP. 36 h after transfection with control or WRN siRNA, HeLa cells were treated with 200 μM H_2O_2 for 20 min and allowed to recover in complete medium. Lysates were prepared at indicated time points following treatment and PARP activation was determined by the intensity of poly-ADP(ribose) (PAR) signal using Western blot analyses; both short and long exposure of Western blot are shown. WRN-depleted cells show increased PAR signal in untreated condition as compared to control siRNA-transfected cells (lane 1 vs. lane 5). WRN-depleted cells show a reduction in further PAR formation following H_2O_2-treatment as compared to control cells (lane 2 vs. lane 6). Depletion of WRN in the lysates was verified by Western blot and is indicated. GAPDH signal in the same blot serves as loading control.

Supplementary Figure 5. BLM-depleted cells display reduced HR efficiency and are sensitive to PARP inhibitor. *A.* DR-U2OS cells were transfected with control or BLM siRNA twice. Upon second siRNA transfection (at I-SceI TF), cells were either harvested for Western blot analysis or additionally transfected with pCAGGS (empty vector) or pCABSce (I-SceI expression vector). 48 h after second siRNA transfection (at FACs), cells were harvested for Western analysis or analyzed for GFP fluorescence. Restoration of a functional GFP gene through complete HR was used to determine HR proficiency. %GFP positive cells were quantitated and relative frequencies were determined by normalizing to control siRNA transfected cells. Mean of relative %GFP positive cells and S.E.M. from four independent experiments are shown. Depletion of BLM at I-SceI TF and FACs, indicated by 1 and 2, respectively, was verified by Western blotting and is shown. GAPDH is used as loading control. *B.* BLM-depleted cells are sensitive to PARP inhibitor ANI. Cells transfected with control or BLM siRNA were subjected to continuous exposure to increasing dose of ANI in complete medium and their survival was measured 72 h later by MTS assay. Percentage of control growth was plotted for each data point, representing the mean ± SD of three independent experiments performed in quadruplicate. Ctl, control.

Supplementary Figure 6. PARP inhibitor does not alter total RECQ1 level and the binding of RECQ1 to chromatin in response to H_2O_2 treatment. HeLa cells grown in the presence or absence of ANI (100 μM) for 24 h, were mock-treated or treated with 1 mM H_2O_2 for 20 min. Cells were washed and harvested in cold PBS and total cell lysate was made using RIPA buffer. For subcellular fractionation, equivalent cell pellets were resuspended in 2 packed cell volumes of buffer containing 20 mM Tris–HCl [pH 7.4], 2.5 mM $MgCl_2$, 0.5% (v/v) Nonidet P-40, 1 mM PMSF, 1 mM DTT and protease inhibitors, and incubated on ice for 10 min. Following centrifugation at 10,000 rpm for 2 min, the supernatant was transferred to a new Eppendorf tube and designated the "soluble" fraction containing cytoplasmic proteins. The remaining nuclear pellet was similarly extracted with 2 packed cell volumes of buffer containing 20 mM Tris [pH 8.0], 0.5 M KCl, 1 mM EDTA, 0.75% (v/v) Triton-X100, 10% (v/v) glycerol, 5 mM $MgCl_2$, 1 mM PMSF, 1 mM DTT, and protease inhibitors, and the supernatant obtained was designated the "insoluble" fraction containing chromatin bound proteins. Proteins from each fraction were analyzed by Western blotting.

Supplementary Figure 7. HRDC domain of WRN protein had no direct homology with RECQ1 protein, except for extreme C-terminal SKNTGAKKRKIDDA (14 amino acid) motif of the RECQ1. The alignment of ATP-dependent DNA helicase Q1 [Homo sapiens], Accession: P46063 (RECQ1) and Werner syndrome ATP-dependent helicase [Homo sapiens], Accession: NP_000544.2 (WRN), aligned with ClastW program (http://www.ebi.ac.uk/Tools/msa/clustalw2/).

MAESSDKLYRVEYAKSGRASCK**KCSESIPKDSLR**MAIMVQSPMFDGKVPHWYHFSCFWKV
GHSIRHPDVEVDGFSELRWDDQQK**VKKTAEAGGVTGK**GQDGIGSKAEKTLGDFAAEYAKS
NRSTCKGCMEKIEKGQVR**LSKKMVDPEKPQLGMIDR**WYHPGCFVKNREELGFRPEYSASQ
LKGFSLLATEDKEALKKQLPGVKSEGKRKGDEVDGVDEVAKKKSKKEKDKDSKLEKALKA
QNDLIWNIKDELKKVCSTNDLKELLIFNKQQVPSGESAILDRVADGMVFGALLPCEECSG
QLVFKSDAYYCTGDVTAWTKCMVKTQTPNRKEWVTPKEFREISYLKKLKVKKQDRIFPPE
TSASVAATPPPSTASAPAAVNSSASADKPLSNMKILTLGKLSRNKDEVKAMIEKLGGK**LT**
GTANKASLCISTKKEVEKMNKKMEEVKEANIR**VVSEDFLQDVSASTK**SLQELFLAHILSP
WGAEVKAEPVEVVAPRGKSGAALSKKSKGQVKEEGINKSEKRMKLTLKGGAAVDPDSGLE
HSAHVLEKGGK**VFSATLGLVDIVK**GTNSYYKLQLLEDDKENR**YWIFRSWGRVGTVIGSNK**
LEQMPSKEDAIEHFMKLYEEKTGNAWHSKNFTKYPKKFYPLEIDYGQDEEAVKKLTVNPG
TKSKLPKPVQDLIKMIFDVESMKKAMVEYEIDLQKMPLGKLSKRQIQAAYSILSEVQQAV
SQGSSDSQILDLSNRFYTLIPHDFGMKKPPLLNNADSVQAKVEMLDNLLDIEVAYSLLRG
GSDDSSKDPIDVNYEK**LKTDIKVVDR**DSEEAEIIRKYVKN**THATTHNAYDLEVIDIFK**IE
REGECQRYKPFKQLHNRRLLWHGSR**TTNFAGILSQGLR**IAPPEAPVTGYMFGKGIYFADM
VSKSANYCHTSQGDPIGLILLGEVALGNMYELKHASHISKLPKG**KHSVKGLGK**TTPDPSA
NISLDGVDVPLGTGISSGVNDTSLLYNEYIVYDIAQVNLKYLLKLKFNFKTSLW

Suppl. Figure 1

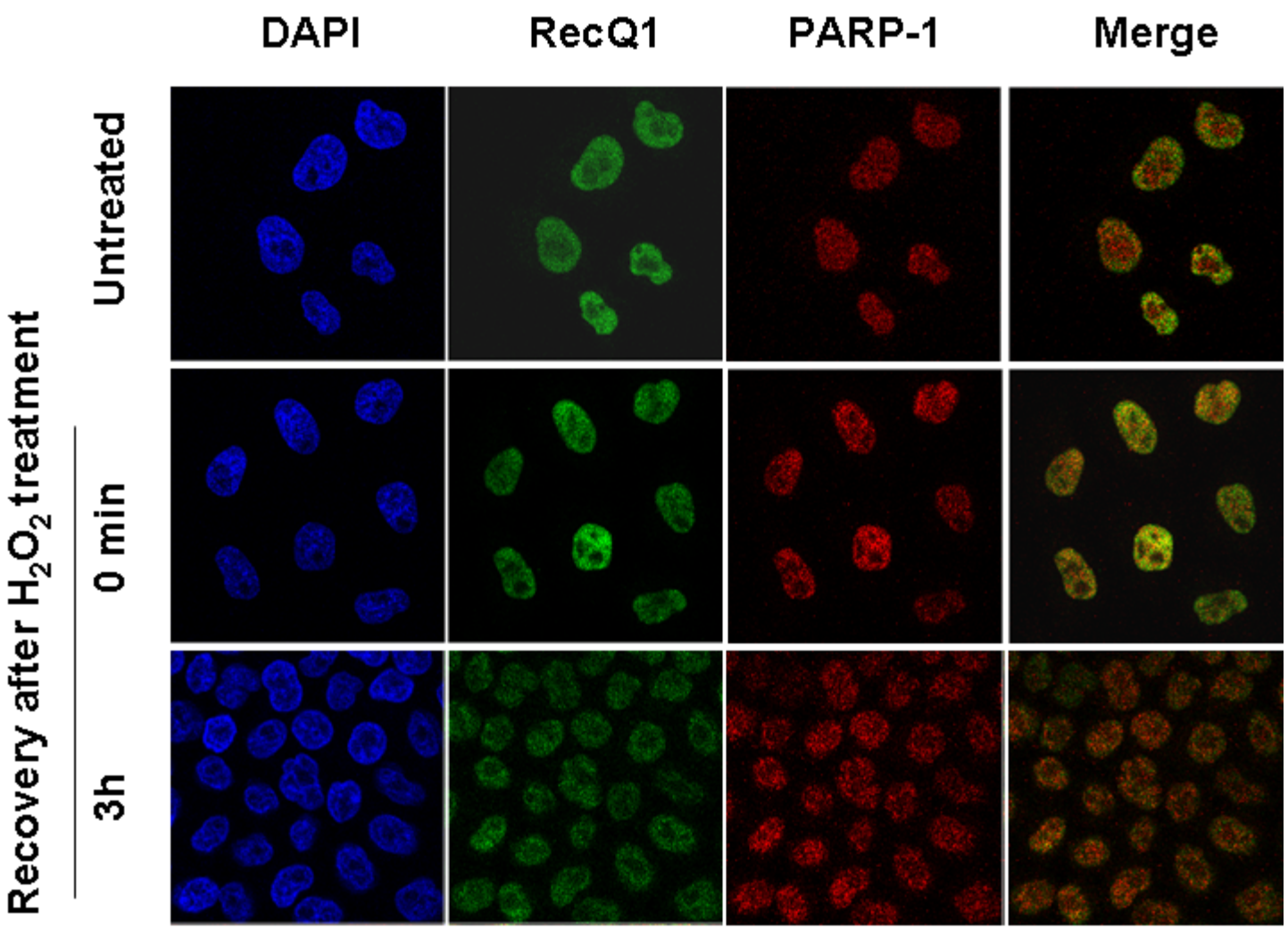

Suppl. Figure 2

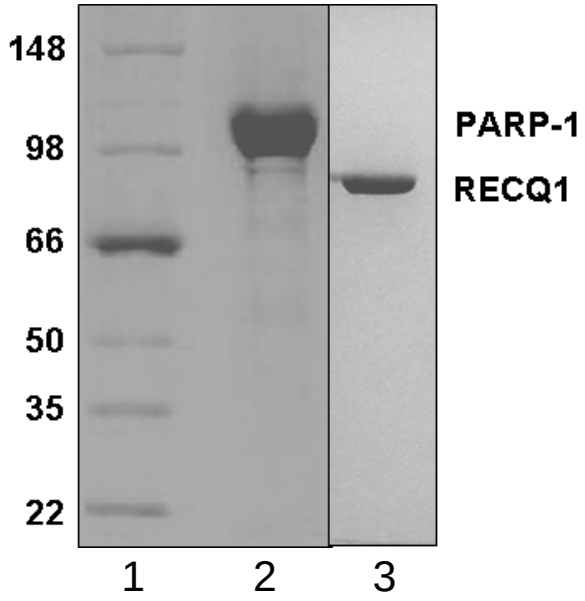

Suppl. Figure 3

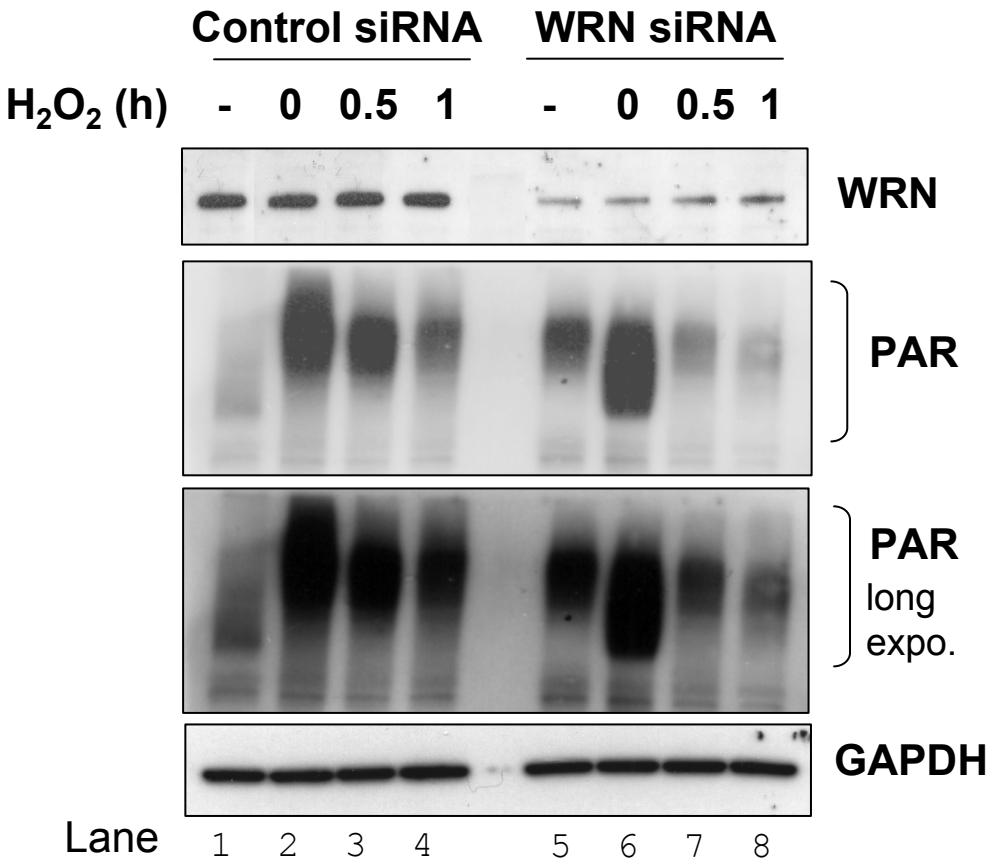

Suppl. Figure 4

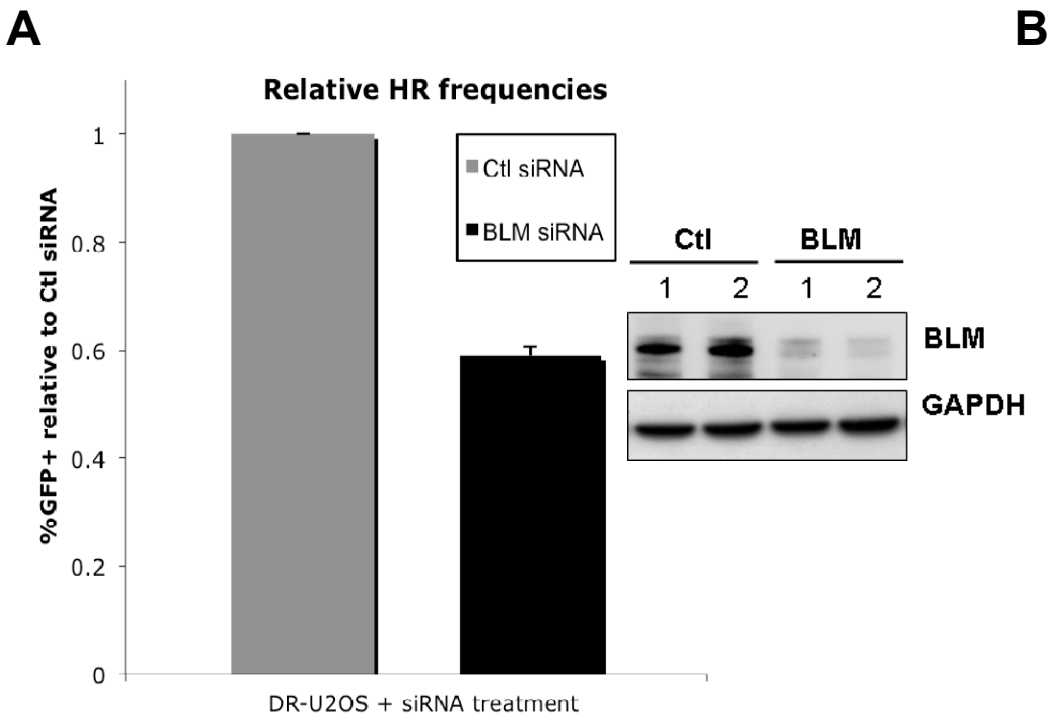

Suppl. Figure 5

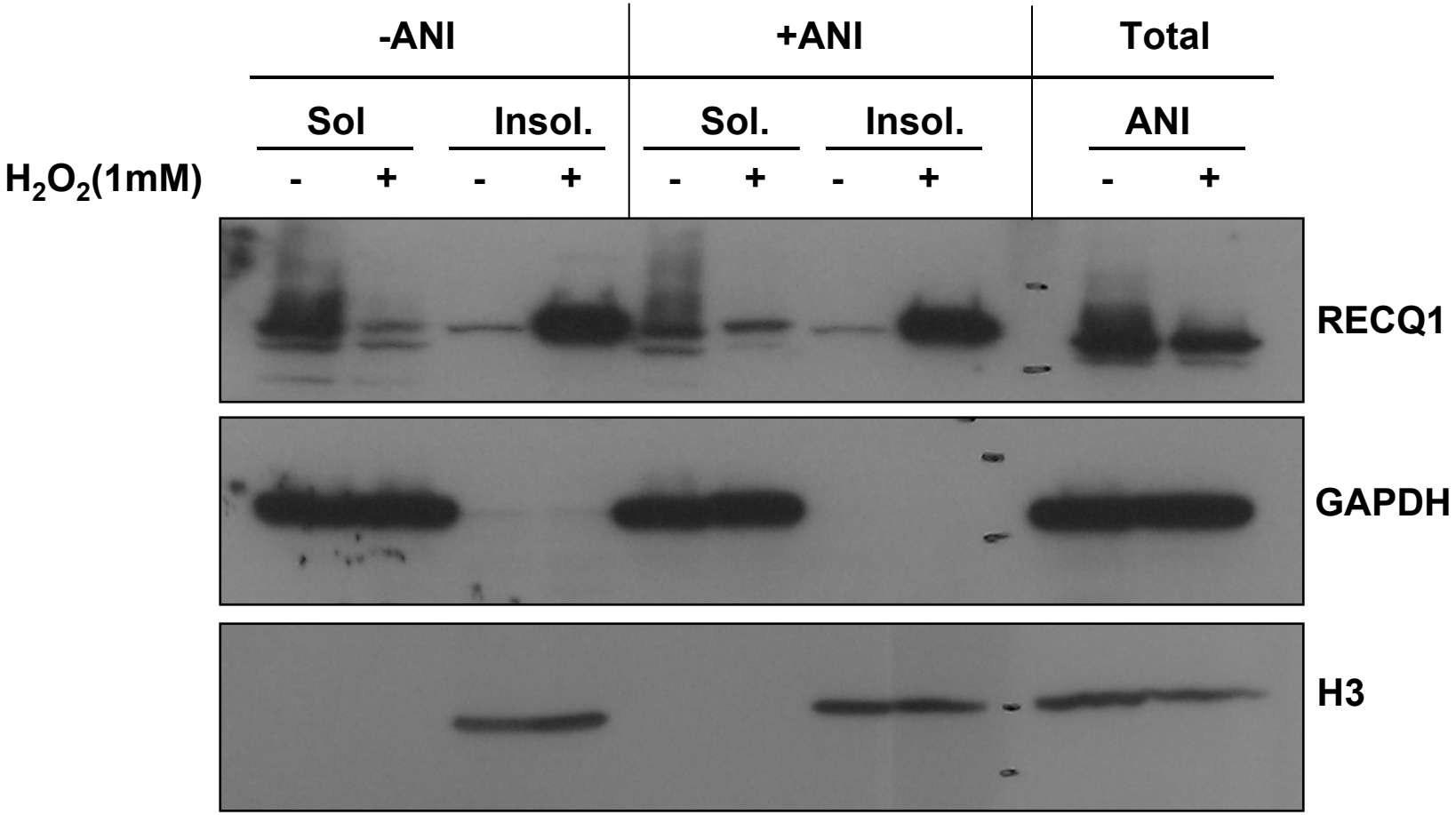

Suppl. Figure 6

Suppl. Figure 7